Internal high-reflectivity omni-directional reflectors

J.-Q. Xi
Future Chips Constellation, Department of Physics, Applied Physics, and Astronomy, Rensselaer Polytechnic Institute, Troy, New York 12180

Manas Ojha, J. L. Plawsky, and W. N. Gill
Department of Chemical and Biological Engineering, Rensselaer Polytechnic Institute, Troy, New York 12180

Jong Kyu Kim and E. F. Schubert[a)]
Future Chips Constellation, Department of Electrical, Computer, and Systems Engineering, Rensselaer Polytechnic Institute, Troy, New York 12180

(Received 28 March 2005; accepted 3 June 2005; published online 15 July 2005)

An internal high-reflectivity omni-directional reflector (ODR) for the visible spectrum is realized by the combination of total internal reflection using a low-refractive-index (low-*n*) material and reflection from a one-dimensional photonic crystal (1D PC). The low-*n* layer limits the range of angles in the 1D PC to values below the Brewster angle, thereby enabling high reflectivity and omni-directionality. This ODR is demonstrated using GaP as ambient, nanoporous SiO_2 with a very low refractive index ($n=1.10$), and a four-pair TiO_2/SiO_2 multilayer stack. The results indicate a two orders of magnitude lower angle-integrated transverse-electric-transverse-magnetic polarization averaged mirror loss of the ODR compared with conventional distributed Bragg reflectors and metal reflectors. This indicates the high potential of the internal ODRs for optoelectronic semiconductor devices, e.g., light-emitting diodes. © *2005 American Institute of Physics*.
[DOI: 10.1063/1.1997270]

It has been known for decades that distributed Bragg reflectors (DBRs) with high-index contrast provide high reflectivity and omni-directionality for low-index *external* mediums (such as air), i.e., for *external* reflection.[1–3] However, such omni-directionality cannot be obtained with DBRs for *internal* reflection, i.e., for reflection in media with a high refractive index such as semiconductors, for the following reasons. First, when used as an internal DBR, the low reflectivity region of transverse magnetic (TM) polarization near the Brewster angle cannot be avoided. Second, due to the high index of the ambient, a small change in incident angle will cause a large change in the optical path length inside each dielectric layer of the DBR. As a result, constructive interference for the reflected wave turns into destructive interference. Inspection of Fig. 1, showing the internal and external reflectance of a high-contrast DBR, elucidates the unattainability of an internal omni-directional reflector (ODR). Metal reflectors are the oldest known ODRs. However, the reflectivity of metals is not high enough, typically 90%–95% in the visible spectral range when the external medium is a high-refractive-index (high-*n*) material. An *internal* ODR with high reflectivity for both transverse electric (TE) and TM polarizations at any angle of incidence has not yet been demonstrated. However there is an urgent need for such reflectors to reduce optical losses in semiconductor light-emitting diodes.[4,5]

Here, a high-reflectivity internal ODR for the visible spectrum is demonstrated, with GaP being the internal medium in which reflection is to occur. The ODR is based on a TiO_2/SiO_2 multilayer stack and a thick low-refractive-index (low-*n*) material located between the high-*n* ambient and the multilayer stack. Figure 2(a) shows the schematic structure of the internal ODR. TiO_2/SiO_2 has one of the highest possible index contrasts in the visible spectrum and both materials are transparent. The refractive indices of the materials at 633 nm are: $n_{GaP}=3.31$, $n_{TiO_2}=2.67$, and $n_{SiO_2}=1.456$. Nanoporous SiO_2[6–9] with an unprecedented low-refractive index of $n_{low}=1.10$ serves as the low-*n* material. Nano-size porosity (average pore size 4 nm) ensures low light-scattering losses.

The internal ODR can be considered to have two high reflectivity regions, one of them being a total internal reflection (TIR) region for incident angles $\theta > \theta_c$, where $\theta_c = \sin^{-1}(n_{low}/n_{GaP}) = 19.4°$ is the critical angle for total internal reflection between the GaP and the low-*n* material. The other region is the reflection from the TiO_2/SiO_2 multilayer stack for incident angles $\theta \leqslant \theta_c$ in the GaP. The low-*n* material

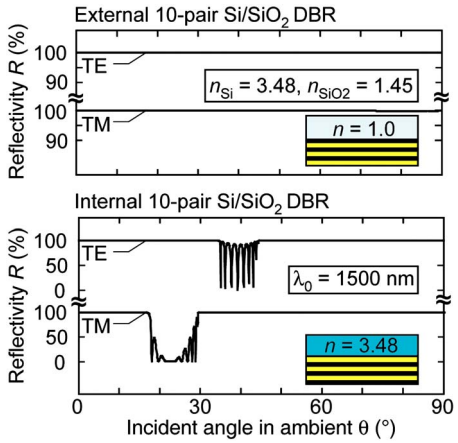

FIG. 1. (Color online) Calculated Si/SiO_2 DBR reflectivity with air ambient (external reflector) and semiconductor ambient (internal reflector) vs angle.

[a)]Author to whom correspondence should be addressed; electronic mail: efschubert@rpi.edu

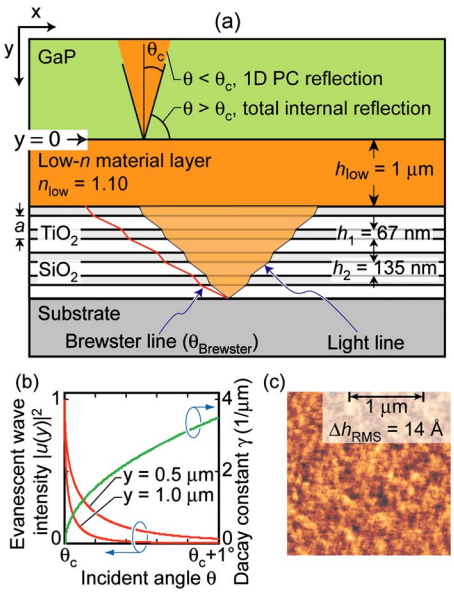

FIG. 2. (Color online) (a), Schematic of internal ODR with high-index ambient (GaP) and nanoporous SiO_2 as low-n material. Total internal reflection region and 1D photonic crystal (TiO_2/SiO_2) reflection region are indicated. Brewster angle is beyond the maximum angle of the light distribution inside the TiO_2/SiO_2 multilayer stack. (b) Angular dependent evanescent wave intensity and decay constant inside low-n material, (c) Atomic force micrograph of a 1.05 μm nanoporous SiO_2 after annealing at 550 °C.

must have a low-refractive index to yield a wide-angle TIR region and to serve as a low-index ambient for the TiO_2/SiO_2 one-dimensional photonic crystal (1D PC).

The low-n material must have a minimum thickness to have good TIR for $\theta > \theta_c$. Due to the finite thickness of the low-n layer, an evanescent wave penetrates through the low-n material and reaches the TiO_2/SiO_2 multilayer stack within the small range of incident angles near the critical angle, i.e., at θ_c to $\theta_c + \Delta\theta$. The evanescent wave field amplitude[10] inside low-n material is given by $u(y) \propto \exp(-\gamma y)$, with y being the distance in the low-n layer from the GaP interface and γ being the decay constant

$$\gamma = n_{\text{low}} k_0 \left(\frac{\sin^2 \theta}{\sin^2 \theta_c} - 1 \right)^{1/2}, \quad \theta_c \leqslant \theta \leqslant \pi/2, \tag{1}$$

where θ and $k_0 = 2\pi/\lambda_0$ are the incident angle inside GaP and the wave vector, respectively. The angular dependent evanescent wave intensity, $|u(y)|^2$, and decay constant, γ, are shown in Fig. 2(b) for different depths inside the low-n material. The thickness of the low-n layer is chosen sufficiently thick (1.0 μm), so that the effect of the evanescent wave reaching the 1D PC can be neglected.

In the case of $\theta \leqslant \theta_c$, all of the light from GaP ambient will propagate through low-n material and reach the TiO_2/SiO_2. A 1D PC analysis is introduced. The light distribution for $\theta \leqslant \theta_c$ is indicated in Fig. 2(a). Due to the large thickness of the low-n layer, the TiO_2/SiO_2 can be regarded as a 1D PC with low-n material as ambient. The photonic band structure and the omni band[11] are shown in Fig. 3. At the light line (solid line in Fig. 3), the parallel wave vector, k_x, and the wave vector, k_0, satisfy the relationship, $k_x = k_0/n_{\text{low}}$ ($n_{\text{low}} = 1.10$). This condition is different from the condition $k_x = k_0$ (dashed line in Fig. 3) required for omni-directionality in *external* ODRs.[1–3] Obviously, the Brewster angle is excluded from the range of angles entering the 1D PC. An omni band

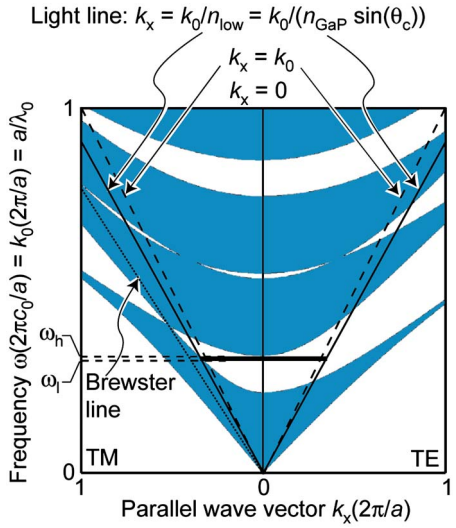

FIG. 3. (Color online) One-dimensional photonic band structure of TiO_2/SiO_2 multilayer stack. Dark area is propagating states and white area is evanescent states. With ambient index $n_{\text{low}} = 1.10$, light line is $k_x = k_0/n_{\text{low}}$, indicating existence of omni band.

between the two light lines is obtained. The bandwidth can be obtained by solving the band-edge equation[1]

$$\frac{1+\Lambda}{2} \cos(k_y^1 h_1 + k_y^2 h_2) + \frac{1-\Lambda}{2} \cos(k_y^1 h_1 - k_y^2 h_2) + 1 = 0, \tag{2}$$

where $k_y^\alpha = \sqrt{(\omega n_\alpha / c_0)^2 - k_x^2}$ ($\alpha = 1, 2$) and

$$\Lambda \equiv \begin{cases} \dfrac{1}{2}\left(\dfrac{k_y^2}{k_y^1} + \dfrac{k_y^1}{k_y^2} \right) & \text{for TE wave} \\ \dfrac{1}{2}\left(\dfrac{n_1^2 k_y^2}{n_2^2 k_y^1} + \dfrac{n_2^2 k_y^1}{n_1^2 k_y^2} \right) & \text{for TM wave.} \end{cases} \tag{3}$$

The omni band is determined by the high frequency, ω_h, and the low frequency, ω_l. The exact solution of ω_h and ω_l can be obtained from Eq. (2) by either a numerical or graphical method, $\omega_h = 2.986 \times 10^{15}$ s^{-1} (631.3 nm), and $\omega_l = 2.951 \times 10^{15}$ s^{-1} (638.8 nm). Thus, the omni-band width is 7.5 nm. The maximum allowed index of the low-n material, $n_{\text{low}}|_{\max}$ that is required to have an omni band can be obtained by numerically solving Eq. (2) under the condition that $\omega_l = \omega_h$, is $n_{\text{low}}|_{\max} = 1.112$. Note that the nanoporous SiO_2 fulfills this requirement but conventional low-n materials (e.g., MgF_2 or dense SiO_2) do not.

The ODR using nanoporous SiO_2 is fabricated as follows. A thin SiO_2 (20 nm) layer is plasma-enhanced chemical-vapor deposited on a 300-μm-thick GaP wafer to change the hydrophobic GaP surface to a hydrophilic SiO_2 surface. This thin layer helps to have good adhesion of spin-coated nanoporous SiO_2 to the GaP. The effect of this SiO_2 thin film on the optical function of the whole device can be neglected. A high-porosity nanoporous SiO_2 film is deposited on the GaP/SiO_2 surface by spin coating a sol-gel solution of tetraethylorthosilicate, ammonium hydroxide (NH_4OH), ethanol and glycol to yield a thick (>1 μm) low-n layer.[6] A dual solvent approach,[7] using ethanol and ethylene glycol, is used to control the film thickness and the porosity independently of one another. An adhesion promoter, Dow-AP8000, is spin coated prior to the coating of high-porosity nano-

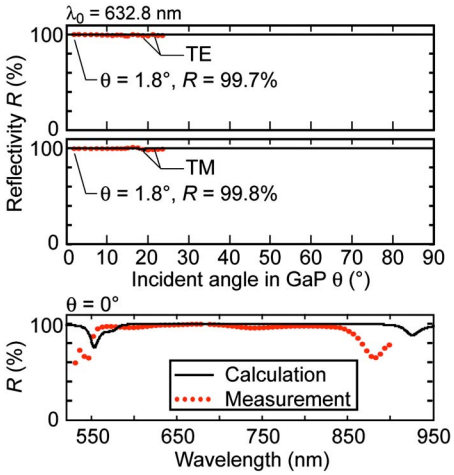

FIG. 4. (Color online) Angular and spectral dependence of measured and calculated reflectivity for internal ODR. The calculated angle-averaged reflectivity is $R_{avg}>99.95\%$ for both the TE and TM polarization.

porous SiO_2. The as-deposited nanoporous SiO_2 has the thickness $h=1166$ nm and index $n=1.12$ at 633 nm. Annealing at 550 °C under 10^{-6} Torr for 2 h stabilizes the thickness and the refractive index of the nanoporous SiO_2 at $h=1052$ nm and $n_{low}=1.10$. Furthermore, the surface becomes smoother by the annealing. Figure 2(c) shows an atomic force micrograph of the nanoporous SiO_2, indicating the excellent surface morphology of the film. The surface roughness is $\Delta h_{rms}=14$ Å. Subsequently, four pairs of 67 nm TiO_2 and 135 nm SiO_2 are deposited on nanoporous SiO_2 using electron-beam evaporation. The TiO_2 deposition is a reactive e-beam evaporation[12] at a substrate temperature of $T=550$ °C and oxygen partial pressure of 2×10^{-4} Torr with the starting source material Ti_3O_5. The SiO_2 is deposited at the same temperature.

A He–Ne laser is used as the light source for the angular dependent internal reflectivity measurement. A high-refractive-index prism ($n=1.778$) and a high-index fluid ($n=1.662$) are used to couple light into the GaP at higher angles of incidence.[13] This method extends the measurable internal reflectivity with angle θ inside the GaP to 23.5°, which is beyond the critical angle of GaP/air interface, 17.6°. Spectral reflectivity at normal incidence is measured with a JASCO V-570 spectrophotometer.

The measurement and calculation results of our internal ODR are shown in Fig. 4. Excellent agreement between the measurement and the calculation is obtained. The calculated reflectivity shown in Fig. 4 demonstrates that the internal ODR has very high reflectivity at any incident angle inside the GaP for both polarizations. The calculated angle-integrated TE-TM averaged reflectivity is $R_{avg}>99.95\%$ which implies a two orders of magnitude lower mirror loss than conventional metal mirrors (typically $R_{avg}=90\%$–95%) or DBRs (typically $R_{avg}=95\%$). Note that a further increase of the omni bandwidth can be achieved by including an additional Ag substrate beneath the TiO_2/SiO_2 multilayer stack due to the fact that Ag has broad omni bandwidth with high reflectivity in the visible spectrum.

In conclusion, a high-reflectivity internal ODR consisting of a GaP high-index ambient, a low-n layer (nanoporous SiO_2), and a TiO_2/SiO_2 multilayer stack is demonstrated. Thick nanoporous SiO_2 layers with an unprecedented low refractive index ($n=1.10$) are a key part of the reflector. Both the measurement and calculation show that our internal reflector has high reflectivity with omni-directionality. The calculated angle-integrated TE-TM averaged reflectivity is $R_{avg}>99.95\%$ which implies a two orders of magnitude lower mirror loss than conventional metal mirrors or DBRs.

The authors gratefully acknowledge support from the National Science Foundation (NSF), the Defense Advanced Research Projects Agency (DARPA), the Army Research Office (ARO), Samsung Advanced Institute of Technology (SAIT), and the Rensselaer Polytechnic Institute (RPI).

[1] Y. Fink, J. N. Winn, S. Fan, C. Chen, J. Michel, J. D. Joannopoulos, and E. L. Thomas, Science **282**, 1679 (1998).
[2] M. Deopura, C. K. Ullal, B. Temelkuran, and Y. Fink, Opt. Lett. **26**, 1197 (2001).
[3] J. N. Winn, Y. Fink, S. Fan, and J. D. Joannopoulos, Opt. Lett. **23**, 1573 (1998).
[4] Th. Gessmann, E. F. Schubert, J. W. Graff, K. Streubel, and C. Karnutsch, IEEE Electron Device Lett. **24**, 683 (2003).
[5] J. K. Kim, Th. Gessmann, H. Luo, and E. F. Schubert, Appl. Phys. Lett. **84**, 4508 (2004).
[6] S. V. Nitta, V. Pisupatti, A. Jain, P. C. Wayner, Jr., W. N. Gill, and J. L. Plawsky, J. Vac. Sci. Technol. B **17**, 205 (1999).
[7] A. Jain, S. Rogojevic, S. Ponoth, N. Agarwal, I. Matthew, W. N. Gill, P. Persans, M. Tomozawa, J. L. Plawsky, and E. Simonyi, Thin Solid Films **398-399**, 513 (2001).
[8] A. Jain, S. Rogojevic, W. N. Gill, and J. L. Plawsky, J. Appl. Phys. **90**, 5832 (2001).
[9] A. Jain, S. Rogojevic, S. Ponoth, W. N. Gill, and J. L. Plawsky, J. Appl. Phys. **91**, 3275 (2002).
[10] B. E. A. Saleh and M. C. Teich, *Fundamentals of Photonics* (Wiley, New York, 1991), p. 253.
[11] P. Yeh, A. Yariv, and C.-S. Hong, J. Opt. Soc. Am. **67**, 423 (1977).
[12] H. K. Pulker, G. Paesold, and E. Ritter, Appl. Opt. **15**, 2986 (1976).
[13] J.-Q. Xi, M. Ojha, W. Cho, J. L. Plawsky, W. N. Gill, Th. Gessmann, and E. F. Schubert, Opt. Lett. **30**, 1518 (2005).